CORE
Metadata, citation and similar papers at core.ac.uk
Provided by Elsevier - Publisher Connector
Immunity, Vol. 14, 315–329, March, 2001, Copyright ©2001 by Cell Press

Dynamic Actin Polymerization Drives T Cell Receptor–Induced Spreading: A Role for the Signal Transduction Adaptor LAT

Stephen C. Bunnell,* Veena Kapoor,* Ronald P. Trible,* Weiguo Zhang,† and Lawrence E. Samelson*‡
*Laboratory of Cellular and Molecular Biology
Division of Basic Sciences
National Cancer Institute
Bethesda, Maryland 20892
†Department of Immunology
Duke Medical Center
Durham, North Carolina 27710

Summary

T cell activation induces functional changes in cell shape and cytoskeletal architecture. To facilitate the collection of dynamic, high-resolution images of activated T cells, we plated T cells on coverslips coated with antibodies to the T cell receptor (TCR). Using these images, we were able to quantitate the morphological responses of individual cells over time. Here, we show that TCR engagement triggers the formation and expansion of contacts bounded by continuously remodeled actin-rich rings. These processes are associated with the extension of lamellipodia and require actin polymerization, tyrosine kinase activation, cytoplasmic calcium increases, and LAT, an important hematopoietic adaptor. In addition, the maintenance of the resulting contact requires sustained calcium influxes, an intact microtubule cytoskeleton, and functional LAT.

Introduction

The engagement of the T cell antigen receptor (TCR) triggers signaling cascades required for T cell activation and the generation of functional immune responses (Chan and Shaw, 1996; Wange and Samelson, 1996; Zhang and Samelson, 2000). These cascades are initiated by Src-, Syk-, and Tec-family protein tyrosine kinases (PTKs) that cooperate to phosphorylate the TCR and various effector molecules. One of these effector proteins, the adaptor LAT, is present in lipid rafts and provides docking sites for the formation of several critical signaling complexes (Finco et al., 1998; Zhang et al., 1998a, 1998b). Once phosphorylated, LAT binds directly to phospholipase Cγ1 (PLCγ1) and the adaptor proteins Grb2 and Gads (Zhang et al., 2000). Phosphorylated LAT also recruits the adaptor SLP-76 through its interaction with Gads (Liu et al., 1999). SLP-76 provides docking sites for additional proteins, including the guanine nucleotide exchange factor (GEF) Vav, the serine-threonine kinase Pak, and the actin-polymerization regulating proteins WASP and Fyb/SLAP (Wu et al., 1996; Bubeck Wardenburg et al., 1998; Krause et al., 2000). Phosphatidylinositol 3′-kinase (PI3K), the Ras-GEF SOS, and the Tec-family tyrosine kinase Itk have also been identified in LAT-containing complexes (Zhang et al., 1998a; Shan and Wange, 1999). These LAT-nucleated complexes are essential for T cell activation, as the phosphorylation of SLP-76, Vav, Itk, and PLCγ1, the induction of calcium influxes, and the activation of extracellular regulated kinases (ERKs) all require the expression of LAT (Finco et al., 1998; Shan and Wange, 1999; Zhang et al., 1999b). Collectively, these LAT-associated proteins regulate several transcription factors, coupling TCR ligation to the transcriptional events associated with T cell activation.

TCR engagement also controls cytoskeletal rearrangements that influence and accompany T cell activation (Dustin and Cooper, 2000). Two observations underscore the importance of the actin cytoskeleton in T cell activation. First, actin polymerization-inhibiting agents can terminate ongoing signaling through the TCR (Valitutti et al., 1995). Second, the loss of WASP, a regulator of actin polymerization, impairs T cell activation and results in a severe T cell immunodeficiency (Derry et al., 1994; Symons et al., 1996; Zhang et al., 1999a). TCR-mediated changes in the actin cytoskeleton have been proposed to govern T cell activation by several mechanisms. First, TCR-directed actin polymerization is required for the formation of extensive contacts between T cells and antigen-presenting cells (APCs) (Delon et al., 1998). Second, polymerized actin may act as a scaffold for the further assembly and stabilization of signaling complexes (Dustin and Cooper, 2000). Third, contractile forces resulting from the myosin-dependent movement of actin filaments may contribute to T cell activation by segregating engaged TCRs into central supramolecular activation clusters (c-SMACs) (Monks et al., 1998; Grakoui et al., 1999). The microtubule cytoskeleton also plays an important role in the generation of immune responses by polarizing toward stimulatory APCs and promoting the targeted delivery of cytokines to these APCs (Kupfer et al., 1994).

Several studies have addressed the biochemical mechanisms that control TCR-dependent cytoskeletal rearrangements. In these studies, polarizing stimuli were provided by APCs, supported lipid bilayers, or immobilized antibodies. In each case, TCR ligation induced events characteristic of early T cell activation, such as the formation of extensive contact surfaces and the polarization of the T cell cytoskeleton (Stowers et al., 1995; Lowin-Kropf et al., 1998; Wulfing et al., 1998; Sedwick et al., 1999). PTKs immediately downstream of the TCR, including the Src-family kinase Lck and the Syk-family kinase ZAP-70, were also implicated in the rearrangement of the T cell cytoskeleton (Delon et al., 1998; Lowin-Kropf et al., 1998). Downstream of these PTKs, the adaptor protein SLP-76 was revealed to play a role in the polymerization of actin (Bubeck Wardenburg et al., 1998). SLP-76-associated effectors were also shown to control the T cell cytoskeleton. In particular, Vav activated the Rho-family GTPases Rac and Cdc42, which governed the extension of lamellipodia and the polariza-

‡To whom correspondence should be addressed (e-mail: samelson@helix.nih.gov).

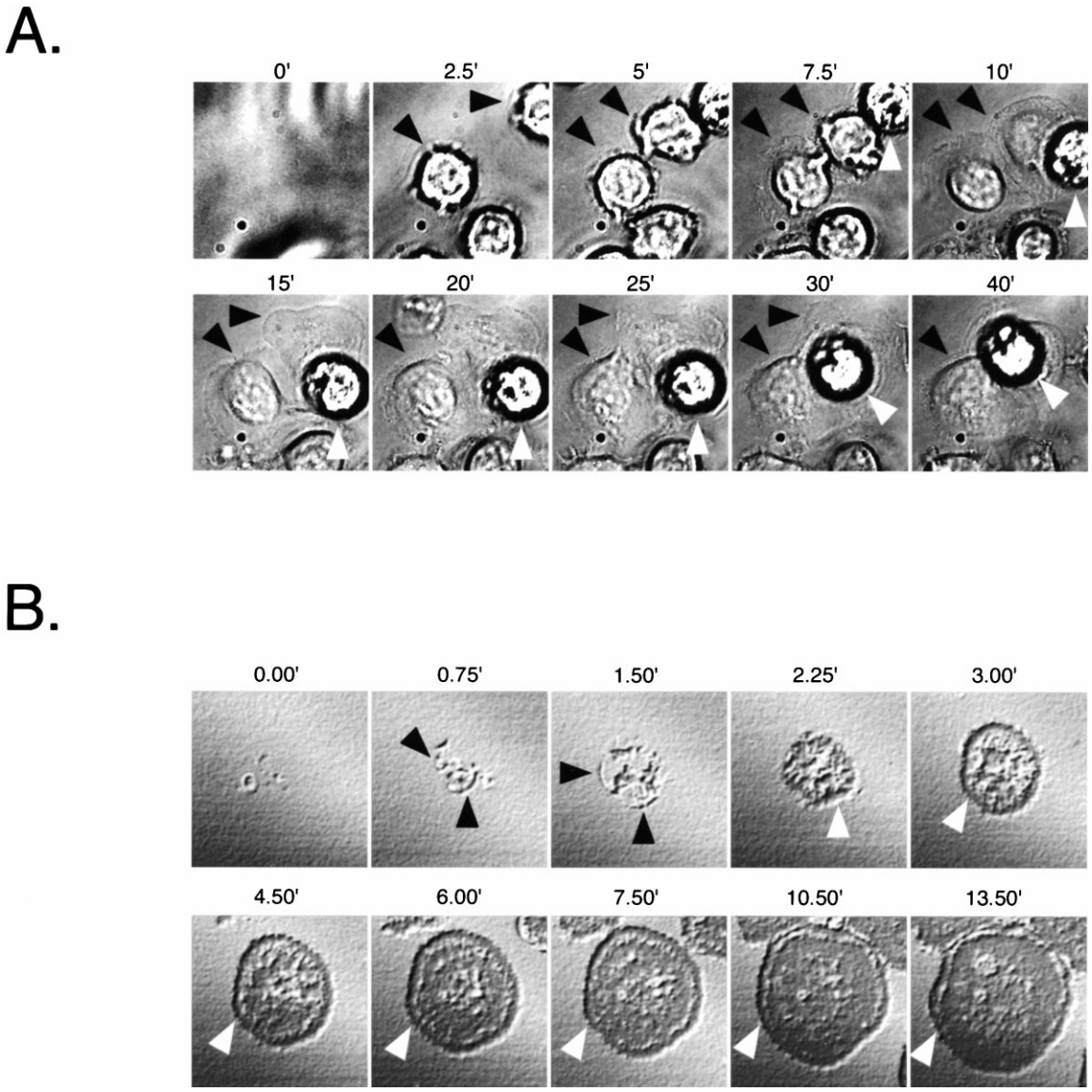

Figure 1. Contact Formation Is Induced by Antibodies to the TCR

(A) Jurkat cells were plated on coverslips coated with the TCR-specific antibody OKT3. Transmitted light images were collected every 15 s using a CCD-equipped epifluorescence microscope. Time was measured from the addition of cells. Black arrows mark cells flattening dramatically over the indicated time course. White arrows mark a nonresponsive cell resting on previously flattened cells, rather than on the coverslip.

(B) Jurkat cells were plated on coverslips coated with the TCR-specific antibody OKT3. Confocal IRM images were collected every 45 s. Darker areas are more closely apposed to the coverslip. Images have been shadowed to increase contrast. Time was measured from the initial contact between the T cell and coverslip. Black arrows indicate contacts formed by the tips of lamellae extended by the responding cell. These contacts mature into a circumferential structure tightly apposed to the coverslip (white arrows).

tion of the microtubule cytoskeleton, whereas WASP, Fyb/SLAP, and Pak controlled the polymerization and stabilization of actin filaments (Stowers et al., 1995; Cantrell, 1998; Edwards et al., 1999; Nobes and Hall, 1999; Krause et al., 2000; Zigmond, 2000). However, to date no studies have addressed the function of LAT with respect to the cytoskeletal changes induced by TCR ligation.

We expected LAT to contribute to TCR-dependent morphological changes by regulating SLP-76 and Vav and through its effects on intracellular calcium levels and ERK activity. Since T cells lacking LAT do not develop in vivo, we used Jurkat T cells to determine the role of LAT with respect to these TCR-induced changes in T cell morphology (Zhang et al., 1999c). To this end, we developed a stimulation assay that enabled us to quantitate the morphological responses of individual Jurkat T cells over time. These morphological changes were monitored by imaging the contact itself using interference reflection microscopy (IRM) and by tracking the distribution of enhanced green fluorescent protein-tagged actin (EGFP-actin) within the responding cells. Using this

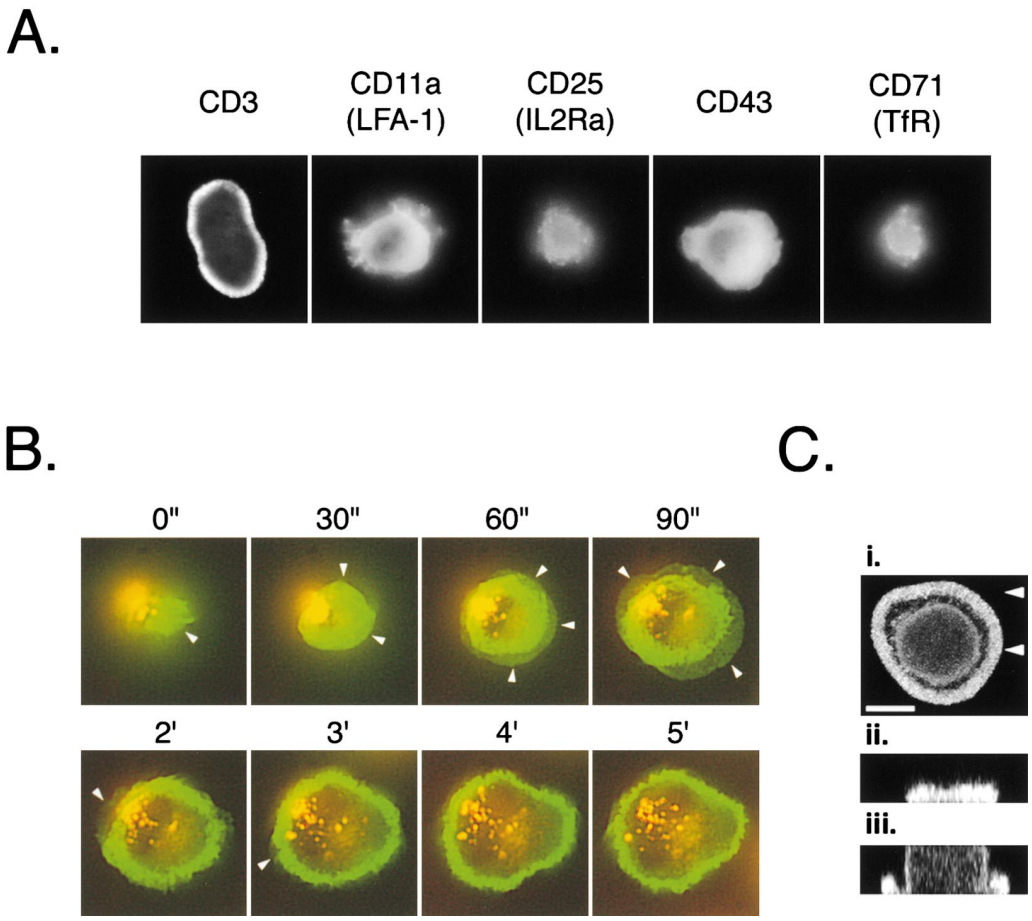

Figure 2. Dynamic Remodeling of the Actin Cytoskeleton during TCR-Induced Spreading

(A) Jurkat cells expressing EGFP-actin were plated on coverslips coated with the indicated antibodies. EGFP-actin was imaged at the coverslip every 30 s using the CCD-equipped microscope. The images presented here were acquired 5 min after the initial contact with the coverslip.

(B) Jurkat cells expressing EGFP-actin were labeled with DiI, plated on coverslips coated with the TCR-specific antibody UCHT1, and imaged every 7.5 s using the CCD-equipped microscope. Time was measured from the initial contact with the coverslip. EGFP-actin is shown in green. The membrane stain DiI appears yellow orange (see Experimental Procedures) and is not relevant to this discussion. White arrows mark large, sheet-like lamellipodia.

(C) EGFP-actin-expressing Jurkat cells were plated on coverslips coated with UCHT1 for 5 min and fixed. Confocal images of EGFP-actin spanning 10 μm of height were collected at 0.5 μm intervals. The images presented were reconstructed as follows: (i) projection of the z-stack onto a horizontal plane; (ii–iii) vertical slices corresponding the arrows in (i); (ii) cross-section through the actin-rich border; (iii) cross-section through the cell body. One representative cell is shown.

assay system, we demonstrated that the morphological changes induced by TCR ligation are absolutely dependent on protein tyrosine kinases and the actin cytoskeleton, are enhanced by increases in cytoplasmic calcium, and are stabilized by the microtubule cytoskeleton. These changes do not, however, depend on ERKs. Finally, we established that LAT is required for TCR-induced spreading and actin rearrangement.

Results

T Cell Spreading Is Induced by Antibodies to the TCR

Parsey and Lewis (1993) observed that Jurkat T cells spread out upon coverslips coated with TCR-specific antibodies and that this process of T cell spreading is accompanied by the rearrangement of filamentous actin (F-actin) into circumferential rings. More recently, Borroto et al. (2000) reached similar conclusions. However, these authors only examined fixed cells. In order to identify the biochemical processes that drive these TCR-induced morphological changes, we adapted the stimulation protocol used by Parsey and Lewis to permit the dynamic imaging of T cells (see Experimental Procedures). Jurkat cells are initially round and refractile, but, upon contacting coverslips coated with CD3-specific antibodies, flatten and become less refractile (Figure 1A, black arrows). This spreading response is antibody specific, as Jurkat cells plated on poly-L-lysine alone remain round and mobile throughout this time frame (data not shown).

The earliest morphological changes accompanying spreading are difficult to resolve by transmitted light microscopy because the initial contact is obscured by the refraction of light through the cell body. In order to obtain more detailed images of the earliest stages of T cell-coverslip contact formation, we imaged developing

A.

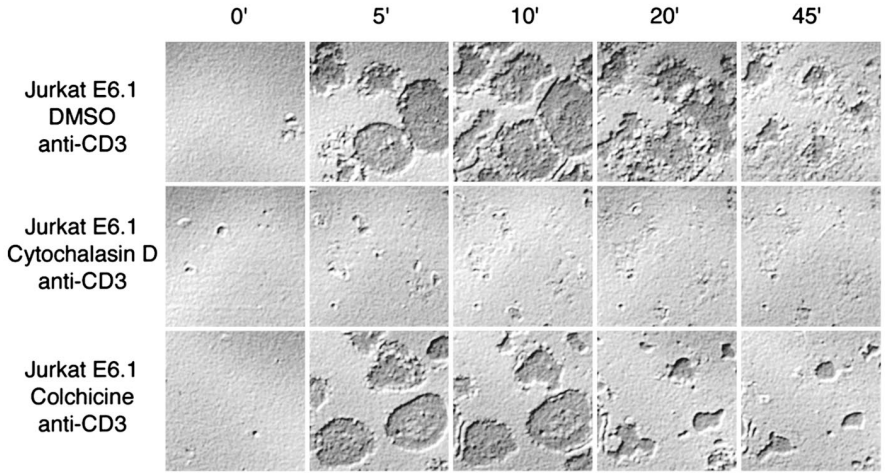
0'
5'
10'
20'
45'
Jurkat E6.1
DMSO
anti-CD3
Jurkat E6.1
Cytochalasin D
anti-CD3
Jurkat E6.1
Colchicine
anti-CD3

B.

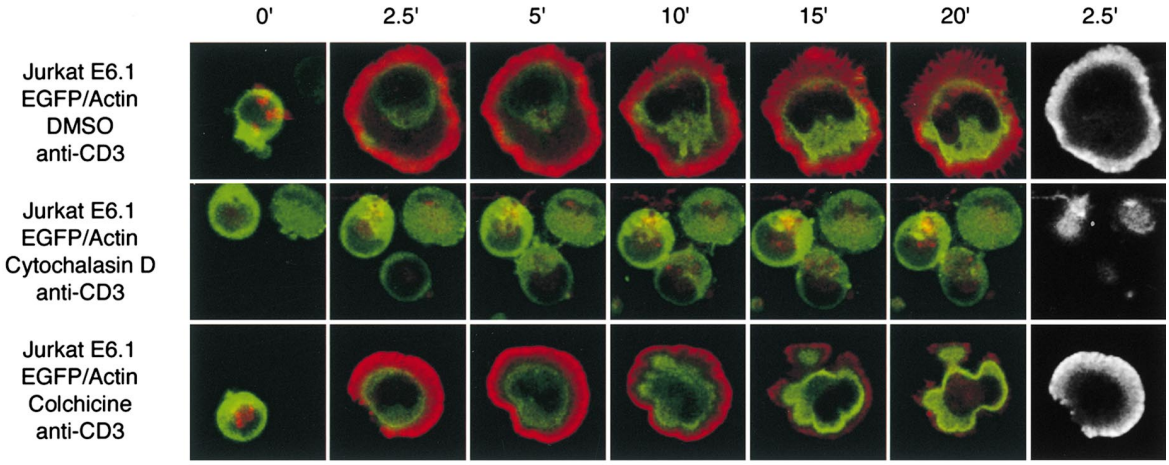
0'
2.5'
5'
10'
15'
20'
2.5'
Jurkat E6.1
EGFP/Actin
DMSO
anti-CD3
Jurkat E6.1
EGFP/Actin
Cytochalasin D
anti-CD3
Jurkat E6.1
EGFP/Actin
Colchicine
anti-CD3

C.

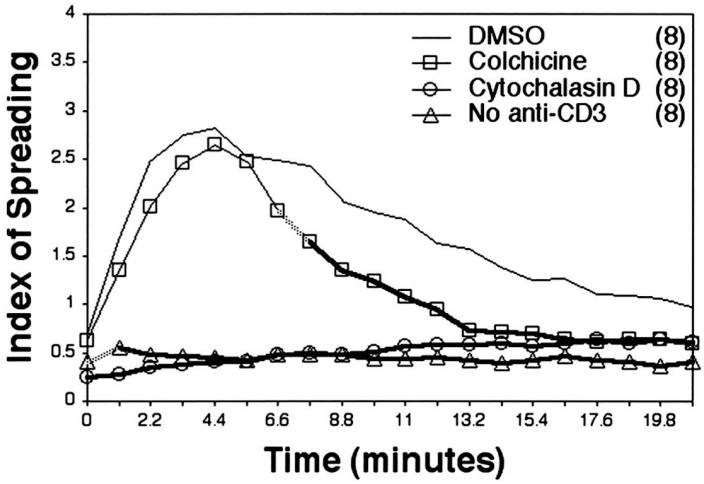
DMSO (8)
Colchicine (8)
Cytochalasin D (8)
No anti-CD3 (8)
Index of Spreading
0
0.5
1
1.5
2
2.5
3
3.5
4
0
2.2
4.4
6.6
8.8
11
13.2
15.4
17.6
19.8
Time (minutes)

contacts using confocal IRM, a method that is based on the fact that cells contacting the coverslip disrupt the coherent reflection of light from the surface of the coverslip. Using this technique, tight contacts appear dark (Figure 1B; see supplemental movie number 1 at http://www.immunity.com/cgi/content/full/14/3/315/DC1). IRM images of the developing contact demonstrate that the interaction between the T cell and the coverslip is initiated by a small filopodial structure ~1 μm in diameter. Shortly after the initiation of contact, lamellipodia project from the responding T cell (data not shown). The tips of these lamellipodia appear in the IRM images as they become apposed to the coverslip (black arrows, 0.75–1.50 min). The contacts initiated by these lamellipodia thicken and merge into a circumferential ring (white arrows, 1.50 min onward) that adheres tightly to the coverslip. The circumferential adherent ring expands over the next 10 min. As this tightly adherent ring moves outward, the T cell continues to flatten against the coverslip, filling the region bounded by the adherent ring. Finally, 15–20 min after the initiation of contact, the outer ring develops gaps and breaks down. The breakdown of this ring is followed by the gradual retraction of the T cell to an irregularly shaped contact that persists for more than 1 hr (see supplemental movie 1 at http://www.immunity.com/cgi/content/full/14/3/315/DC1; data not shown). Again, Jurkat cells plated on poly-L-lyine alone show none of these changes.

TCR Engagement Specifically Triggers Dynamic Remodeling of the Actin Cytoskeleton

The dynamic movement of the circumferential adherent ring suggested its involvement in the expansion of the T cell-coverslip contact. We expected that the actin cytoskeleton would participate in this movement. By allowing Jurkat cells to respond to coverslips coated with CD3-specfic antibodies for 5 min, fixing the cells, and staining with phalloidin, we were able to confirm that F-actin is rearranged into circumferential rings (data not shown). These cytoskeletal structures colocalize with the adherent rings described above, suggesting that the actin-rich ring is also dynamically remodeled. To confirm this hypothesis, we tracked changes in the morphology of the actin-rich ring over time by performing spreading assays with Jurkat cells stably transfected with EGFP-actin (Figure 2A). In these assays, EGFP-actin rearranges into actin-rich rings similar to those observed in fixed cells. Ring formation does not occur in response to immobilized antibodies binding other T cell surface molecules, indicating that this process is specifically controlled by TCR engagement. These differences are also apparent over time (see supplemental movie 2 at http://www.immunity.com/cgi/content/full/14/3/315/DC1).

In order to observe the dynamic changes in the organization of the actin cytoskeleton with greater temporal resolution, we imaged developing contacts using a CCD-equipped microscope (Figure 2B; see supplemental movie 3 at http://www.immunity.com/cgi/content/full/14/3/315/DC1). In these images, EGFP-actin appears as green, and DiI, a membrane label here enriched in vesicular structures, appears as yellow. Initially, T cells contact the coverslip through a small region containing a high density of actin. This contact expands rapidly and in an ordered fashion. First, large, sheet-like lamellipodia extend outward from the contact and along the coverslip (white arrows, 30 s to 2 min). Subsequently, actin accumulates in regions of the contact previously defined by lamellipodia, increasing the diameter of the actin-rich patch, and actin clears from the center of the contact, converting this patch into an actin-rich ring (30 s to 3 min). After 3 min, the expansion of actin ring slows, the frequency with which lamellipodia are extended declines, and the sizes of the lamellipodia extended from the cell decrease (see supplemental movie 3 at http://www.immunity.com/cgi/content/full/14/3/315/DC1). However, the extension of lamellipodia does not cease at this point, as we were able to observe dynamic remodeling of the actin cytoskeleton within persistent circumferential lamellipodia 10–15 min after the initiation of contact (see supplemental movie 4 at http://www.immunity.com/cgi/content/full/14/3/315/DC1). Eventually, 15–20 min after the initiation of contact, the actin-rich ring, like the circumferential adherent ring observed by IRM, develops gaps and breaks down (data not shown). After this point, the T cells retract to cover a smaller area.

Lamellipodia clearly play a role in early T cell spreading, as shown in the IRM and CCD images shown above. However, lamellipodia are much less evident 3 min after the initiation of contact. To determine whether lamellipodia could play a significant role in subsequent morphological events, we examined the three-dimensional distribution of EGFP-actin in Jurkat cells that had been plated on stimulatory coverslips and fixed after 5 min. Top-down projections derived from the resulting confocal image stacks reveal that the actin-rich ring is not uniform but is actually composed of distinct actin-bright structures (Figure 2Ci). Reconstructed cross-sections through the actin-rich ring show that these structures project several micrometers upward from the coverslip (Figure 2Cii), while cross-sections through the cell body demonstrate that these structures project outward from the base of the contact (Figure 2Ciii). These images suggest that the dynamically remodeled actin-rich ring

Figure 3. The Role of the Cytoskeleton in TCR-Induced Spreading

Jurkat cells expressing EGFP-actin were pretreated with cytoskeletal inhibitors and plated onto coverslips coated with the TCR-specific antibody UCHT1. (A) Contacts were imaged by confocal IRM. (B) Confocal EGFP-actin images were obtained at the coverslip and 5 μm above the coverslip every 33 s. For most panels, EGFP-actin at the coverslip is shown in red and EGFP-actin in the cell body is shown in green. The rightmost column contains grayscale images of EGFP actin at the coverslip. Representative cells were chosen based on conformity to the mean behavior depicted below. (C) Mean spreading indices were calculated as described in Experimental Procedures. Line thicknesses indicate the probability of a significant difference from the mean spreading index observed with DMSO-treated cells; dotted or heavy lines, respectively, indicate that the difference achieves a confidence level greater than 95% or 99%. Similar results were obtained in three independent experiments.

A.

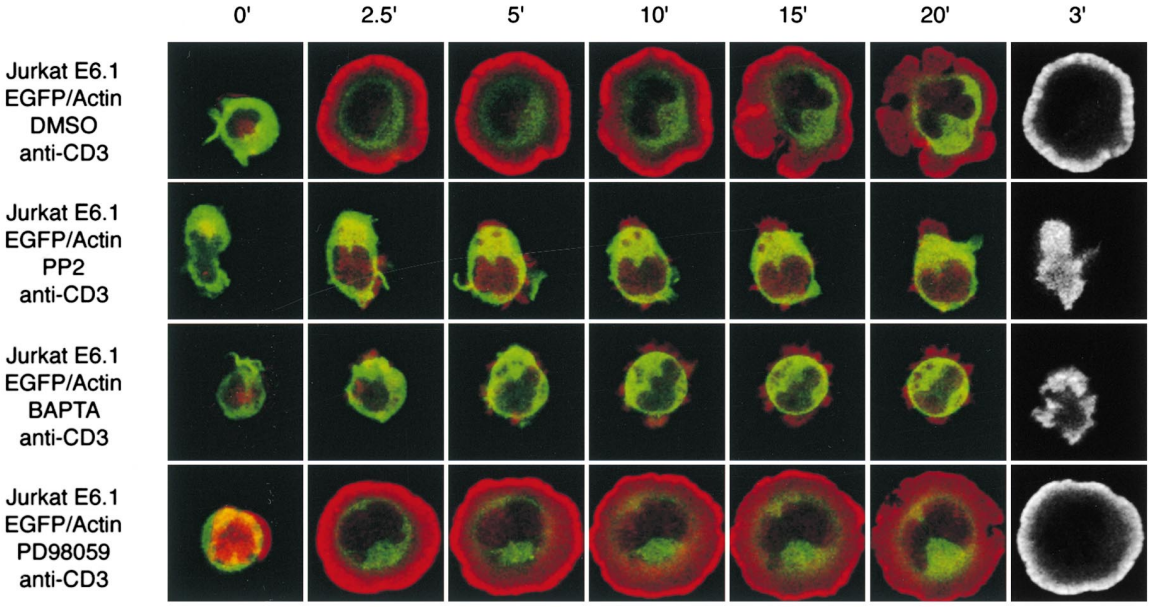
0'
2.5'
5'
10'
15'
20'
3'
Jurkat E6.1
EGFP/Actin
DMSO
anti-CD3
Jurkat E6.1
EGFP/Actin
PP2
anti-CD3
Jurkat E6.1
EGFP/Actin
BAPTA
anti-CD3
Jurkat E6.1
EGFP/Actin
PD98059
anti-CD3

B.

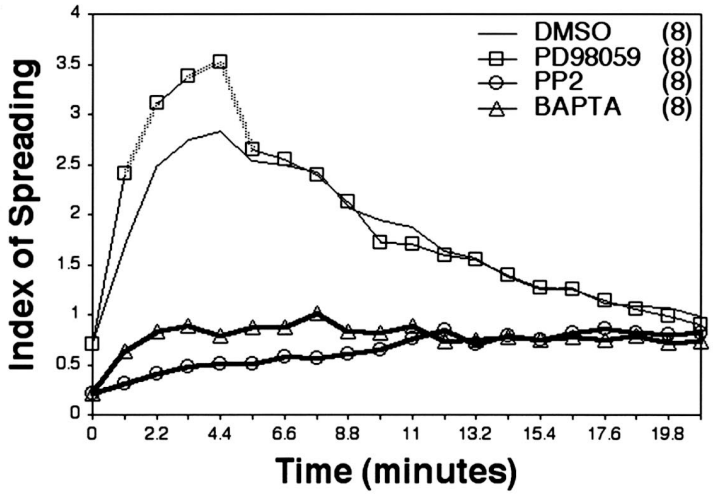
DMSO (8)
PD98059 (8)
PP2 (8)
BAPTA (8)
Index of Spreading
Time (minutes)
0
0.5
1
1.5
2
2.5
3
3.5
4
0
2.2
4.4
6.6
8.8
11
13.2
15.4
17.6
19.8

C.

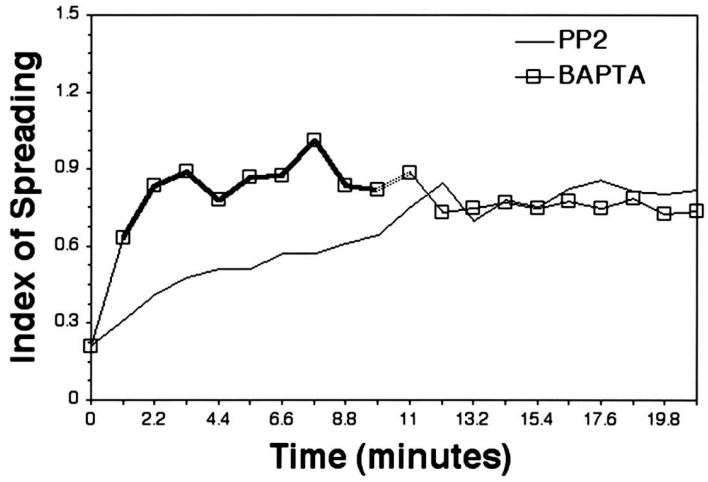
PP2
BAPTA
Index of Spreading
Time (minutes)
0
0.3
0.6
0.9
1.2
1.5
0
2.2
4.4
6.6
8.8
11
13.2
15.4
17.6
19.8

is, at least in part, composed of lamellipodia. Similar structures can be observed in live cells (data not shown).

The Role of the Cytoskeleton in TCR-Induced Spreading

The continuous remodeling of the actin cytoskeleton throughout the formation and stabilization of contacts suggests that the actin cytoskeleton drives T cell spreading. However, the microtubule cytoskeleton has been shown to polarize toward contacts in response to either stimulatory APCs or immobilized TCR-specific antibodies (Kupfer and Dennert, 1984; Lowin-Kropf et al., 1998). We confirmed that the microtubule cytoskeleton repolarizes toward contacts in our assay system using EGFP-tubulin expressing Jurkat T cells (data not shown). Jointly, these observations suggest that the microtubule cytoskeleton also contributes to TCR-induced spreading. To test these hypotheses, we asked whether or not cytochalasin D, an inhibitor of actin polymerization, or colchicine, a microtubule depolymerizing agent, could affect TCR-induced T cell spreading. IRM images revealed that cells treated with carrier alone develop normal adhesive contacts (Figure 3A, upper row). In contrast, cytochalasin D-treated cells do not adhere tightly to the coverslip, and the loose contacts formed under these conditions do not expand in an organized fashion (Figure 3A, second row). Colchicine treatment does not affect the initial phase of contact formation but appears to promote the retraction of treated cells after 10 min (Figure 3A, bottom row).

In order to quantitate changes in cell shape and cytoskeletal organization, we monitored the distribution of actin within stimulated Jurkat T cells. For these assays, T cells stably transfected with EGFP-actin were plated on stimulatory coverslips and imaged at regular intervals for at least 30 min. In each imaging cycle, we obtained confocal images of EGFP-actin at the coverslip (Figure 3B, pseudocolored red) and 5 μm above the coverslip, in the cell body (Figure 3B, pseudocolored green). By comparing these images, we were able to assess the extent of spreading based on three criteria: the size of the contact relative to the size of the cell body (red- versus green-bounded areas), the redistribution of actin from the cell body to the coverslip (red brightness versus green brightness), and the segregation of actin into circumferential rings (shown in red). These factors were incorporated into a spreading index (see Experimental Procedures) which, when plotted against time, graphically depicts the morphological changes observed under various conditions (Figure 3C). Within these charts, statistically significant differences between cell populations are represented by increases in line thickness and weight.

Using this protocol, we examined the spreading responses of Jurkat T cells treated with DMSO carrier (Figure 3B, top row; see supplemental movie 5 at http://www.immunity.com/cgi/content/full/14/3/315/DC1). Within 2.5 min, these cells develop contacts greater in size than the cell body (red- versus green-bounded areas). Within a similar time frame, EGFP-actin translocates extensively from the cell body to the contact (increased red brightness and decreased green brightness). EGFP-actin at the coverslip is also rapidly remodeled into actin-rich circumferential rings, shown in red, or, for clarity, as an isolated grayscale image (right panel). After 5 min, the concentration of actin in the cell body gradually increases as the actin rich ring dissipates and as the distribution of actin at the coverslip becomes more uniform. These changes are reflected in the spreading index, which reaches a maximum 3–5 min after the initiation of contact and gradually declines thereafter (Figure 3C). These responses were indistinguishable from those of untreated Jurkat T cells (data not shown).

We examined the spreading responses of cytochalasin D-treated cells (Figure 3B, second row). Unlike DMSO-treated cells, cytochalasin D-treated cells do not develop large contacts. In addition, in the presence of cytochalasin D, EGFP-actin neither translocates from the cell body to the contact nor segregates into a circumferential region rich in actin (Figure 3B). Similarly, the spreading index of cytochalasin D-treated T cells does not rise to a peak; rather, the spreading index remains flat over time and is similar to the spreading index observed when DMSO-treated cells are plated in the absence of stimulatory antibodies (Figure 3C). The effects of cytochalasin D treatment are highly significant, confirming that the actin cytoskeleton drives TCR-induced spreading.

We also examined the spreading responses of colchicine-treated cells in this manner. EGFP-actin images of the colchicine-treated cells do not reveal any defects in the initial expansion of the contact, the redistribution of actin from the cell body, or the segregation of actin into distinct zones (Figure 3B, bottom row). However, the thinning of the actin ring becomes pronounced within 10 min; after this point, actin quickly redistributes into the cell body and the area of contact declines precipitously. The spreading index of the colchicine-treated cells behaves normally at first, peaking 3–5 min after the initiation of contact, but drops rapidly thereafter. The effects of colchicine treatment do not become statistically significant until ~7 min after the initiation of the contact, confirming that the microtubule cytoskeleton contributes to the maintenance, but not the formation, of T cell-coverslip contacts. (Figure 3C).

Figure 4. Identification of Signaling Pathways Required for TCR-Induced Spreading

Jurkat cells expressing EGFP-actin were pretreated with kinase inhibitors or calcium chelators and plated onto coverslips coated with the TCR-specific antibody UCHT1. (A) Cells were imaged as in Figure 3B. The brightness of EGFP-actin was artificially enhanced in the grayscale images of PP2- and BAPTA- treated cells in order to facilitate the visualization of actin at the contact. (B) Mean spreading indices were calculated as described in Experimental Procedures. Line thicknesses indicate the probability of a significant difference from the mean spreading index observed with DMSO-treated cells; dotted or heavy lines, respectively, indicate that the difference achieves a confidence level greater than 95% or 99%. Similar results were obtained in three independent experiments. (C) Mean spreading indices of cells treated with PP2 or BAPTA (B) were tested for statistically significant differences. Line thicknesses indicate the probability of a significant difference from the mean spreading index observed with PP2-treated cells.

Identification of Signaling Pathways Required for TCR-Induced Spreading

Tyrosine kinases play a critical and early role in the transduction of signals following TCR engagement. Since the Src-family kinases Lck and Fyn are critical mediators of TCR-proximal signaling events, we tested the ability of PP2, which inhibits both Lck and Fyn, to inhibit T cell spreading. As anticipated, PP2 blocks all of the structural changes normally observed upon TCR ligation, including the expansion of the contact, the redistribution of actin to the coverslip, and the segregation of actin into distinct zones at the coverslip (Figure 4A, PP2). The index of spreading accurately reflects these effects (Figure 4B).

In T cells, LAT, SLP-76, Vav, Itk, and PLCγ1 collaborate to regulate intracellular calcium levels by governing the release of calcium from intracellular stores and the influx of calcium across the plasma membrane (Finco et al., 1998; Fischer et al., 1998; Holsinger et al., 1998; Liu et al., 1998; Scharenberg and Kinet, 1998; Yablonski et al., 1998; Costello et al., 1999). Since cytoplasmic calcium elevations release integrins from cytoskeletal constraints, participate in the reorientation of the cortical actin cytoskeleton, and correlate with cell rounding and decreased lamellipodial extension, we wished to test the role of calcium in the regulation of the cytoskeleton by TCR engagement (Negulescu et al., 1996; Stewart et al., 1998; Wulfing and Davis, 1998). In order to completely block TCR-induced calcium elevations, we performed spreading assays in media buffered with EGTA, a calcium chelator, and pretreated cells with BAPTA-AM, a membrane-permeant calcium chelator. These conditions prevent all intracellular calcium elevations and severely perturb the expansion of the contact and the redistribution of actin to the coverslip, resulting in substantial reductions in the spreading index (data not shown; Figures 4A and 4B, BAPTA). However, the small amount of actin present at the coverslip clears from the center of the contact and clusters at the perimeter of the contact (Figure 4A, BAPTA, right panel). This does not occur in PP2-treated cells (Figure 4A, PP2, right panel). To emphasize the effect of this segregation of actin on the spreading index, we replotted the spreading indices associated with PP2-treated and BAPTA-treated cells, revealing a small but significant increase in the spreading indices of BAPTA-treated cells relative to PP2-treated cells (Figure 4C). These observations demonstrate that calcium elevations are required for normal TCR-induced spreading but are not strictly required for the reorganization of actin at the coverslip.

Extracellular regulated kinases, or ERKs, are activated downstream of the TCR by pathways requiring the hematopoietic adaptors LAT and SLP-76. Although ERKs are well known for their ability to govern critical transcriptional responses downstream of the TCR, ERKs have also been reported to enhance actin/myosin-dependent contractility by promoting the phosphorylation of myosin light chain (Cheresh et al., 1999; Fincham et al., 2000). Since MEKs are required for the activation of ERKs, we were able to assess the role of ERKs with respect to T cell spreading by using PD98059, a MEK inhibitor, to block ERK activation (Dudley et al., 1995). ERKs were not required for TCR-induced rearrangements, as the expansion of the contact, the redistribution of actin to the coverslip, and the segregation of actin into distinct zones at the coverslip proceed normally in the presence of PD98059 (Figure 4A). In fact, the spreading index of PD98059-treated cells often peaks at levels exceeding those of DMSO-treated cells (Figure 4B). Thus, the activation of actin/myosin-dependent contractility by ERKs is unlikely to contribute to the morphological changes observed in this assay and may antagonize these changes to a limited extent.

LAT Is Required for TCR-Induced Spreading

LAT is required for the phosphorylation and activation of SLP-76, Vav, Itk, and PLCγ1 in response to TCR-crosslinking (Finco et al., 1998; Shan and Wange, 1999). Collectively, these adaptors and enzymes have been implicated in the control of actin polymerization, the polarization of the microtubule cytoskeleton, and the generation of calcium elevations (referenced above). Thus, we expected LAT to participate in the induction of TCR-dependent morphological changes. In order to test this hypothesis, we assayed the spreading responses of EGFP-actin expressing Jurkat subclones that lack LAT (J.CaM2.5) or have been reconstituted with LAT (J.CaM2.5:WT). As expected, the responses of LAT-reconstituted J.CaM2.5:WT cells are more extensive and less transient than the responses of the J.CaM2.5 cells (Figures 5A and 5B). Although peak levels of spreading persist for somewhat less time in the J.CaM2.5:WT cells than in the parental Jurkat cells, the levels of spreading observed in these cell lines reach similar maxima and stabilize at similar levels (Figures 3C and 5B). Furthermore, the steady-state level of spreading observed in J.CaM2.5:WT cells remains significantly above that observed in J.CaM2.5 cells throughout the assay, indicating that LAT is sufficient to restore most of the morphological responses impaired in J.CaM2.5 cells.

Strikingly, these EGFP-actin images reveal that J.CaM2.5 cells generate significant spreading responses, as assessed by the expansion of the contact, the redistribution of actin to the coverslip, and the segregation of actin into distinct zones at the coverslip. Notably, the transient contacts generated by J.CaM2.5 cells were frequently more irregular in shape than the contacts generated by wild-type or LAT-reconstituted cells (Figure 5A; data not shown). These morpholoical changes were reflected in the spreading index for the J.CaM2.5 cells, which peaked 1 min after the initiation of contact. These observations demonstrate the existence of pathways capable of directing limited spreading responses in the absence of LAT.

LAT Contributes to TCR-Induced Spreading by Calcium-Dependent and Calcium-Independent Pathways

J.CaM2.5 cells spread, albeit transiently, in response to stimulatory coverslips. However, previous reports have established that LAT is required for the production of calcium elevations in response to TCR ligation, and we have shown that calcium elevations are required for TCR-induced spreading. These observations imply that J.CaM2.5 cells must either produce calcium elevations in the absence of LAT or spread in a distinct, calcium-

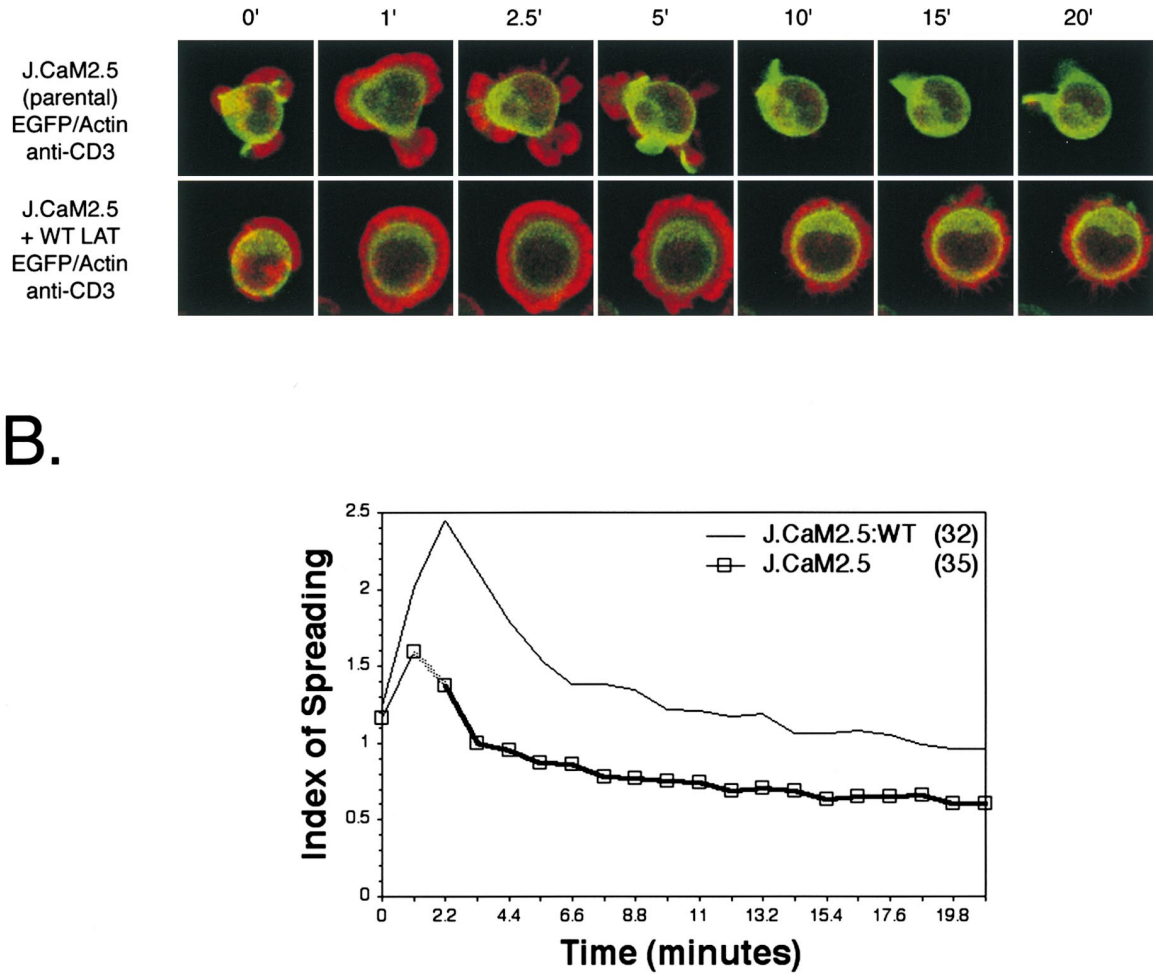

Figure 5. LAT Is Required for TCR-Induced Spreading

J.CaM2.5 cells and J.CaM2.5:WT cells expressing EGFP-actin were plated onto UCHT1-coated coverslips. (A) Confocal EGFP-actin images were obtained at the coverslip and 5 μm above the coverslip every 33 s. EGFP-actin at the coverslip is shown in red; EGFP-actin in the cell body is shown in green. Representative cells were chosen based on conformity to the mean behavior depicted below. (B) Mean spreading indices were calculated as described in Experimental Procedures. Line thicknesses indicate the probability of a significant difference from the mean spreading index observed with J.CaM2.5:WT cells; dotted or heavy lines, respectively, indicate that the difference achieves a confidence level greater than 95% or 99%. Similar results were obtained in six independent experiments.

independent manner. To determine whether or not calcium plays a role in the spreading responses of these cells, we plated J.CaM2.5 cells on stimulatory coverslips in the absence of free extracellular calcium (Figure 6A, EGTA). This treatment prevents calcium influxes and partially inhibits the transient peak of spreading but does not influence spreading after this point. In contrast, when intracellular calcium elevations are prevented by eliminating calcium influxes and buffering intracellular calcium, all spreading is abolished, as in normal Jurkat T cells (Figure 6A, BAPTA). These observations suggest that intracellular calcium elevations are generated when J.CaM2.5 cells contact stimulatory coverslips but are insufficient to sustain T cell spreading. Using intracellular calcium indicators, we confirmed this hypothesis by demonstrating that J.CaM2.5 cells produce small calcium elevations persisting for only 15–20 s in response to stimulatory coverslips (data not shown).

To confirm that calcium is required for the cytoskeletal rearrangements observed in LAT-reconstituted J.CaM2.5 cells, we performed spreading assays under conditions that prevent calcium influxes or prevent all intracellular calcium increases. Calcium influxes begin to significantly affect the sustained spreading responses of LAT-reconstituted J.CaM2.5 cells 12 min after the initiation of contact (Figure 6B, EGTA). As above, intracellular calcium increases are required for both the expansion of the T cell-coverslip contact and sustained spreading (Figure 6B, BAPTA).

In Jurkat T cells, the chelation of intracellular calcium prevents the expansion of the T cell-coverslip contact but permits the clustering of actin within the contact

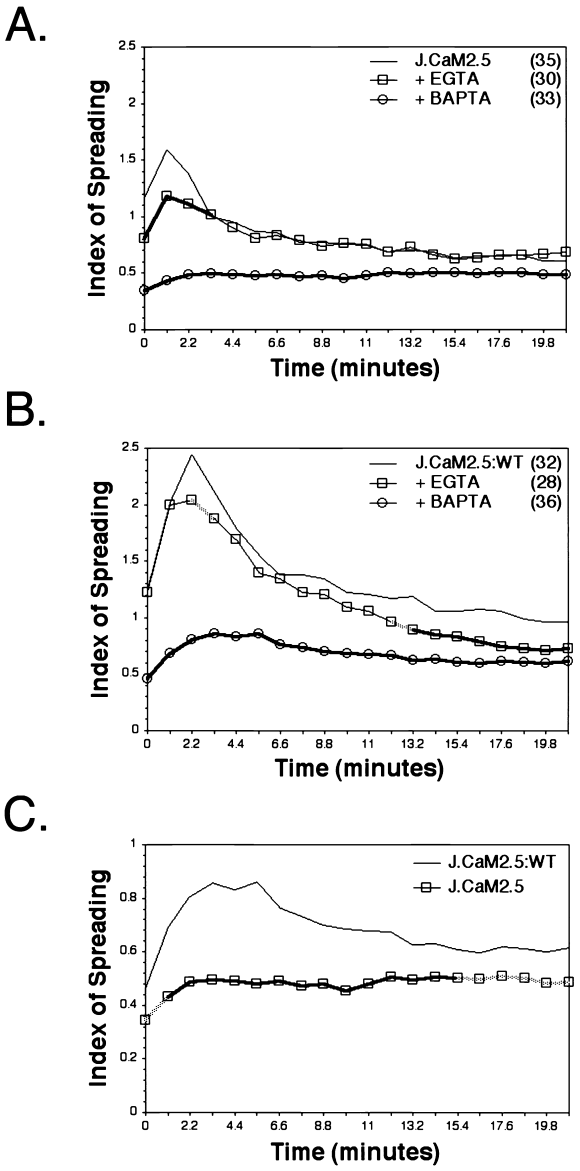

Figure 6. LAT Contributes to TCR-Induced Spreading by Calcium-Dependent and Calcium-Independent Pathways

(A) J.CaM2.5:WT cells expressing EGFP-actin were plated onto UCHT1-coated coverslips. Cells were either pretreated with BAPTA and plated in the presence of EGTA (BAPTA), plated in the presence of EGTA without pretreatment (EGTA), or left untreated. Cells were imaged and analyzed as in Figure 5; mean spreading indices are plotted here. Line thicknesses indicate the probability of a significant difference from the mean spreading index observed for untreated cells; dotted or heavy lines, respectively, indicate that the difference achieves a confidence level greater than 95% or 99%.

(B) J.CaM2.5 cells expressing EGFP-actin were analyzed as above.

(C) Mean spreading indices of BAPTA-treated J.CaM2.5 and J.CaM2.5:WT cells expressing EGFP-actin (see [A] and [B]) were tested for statistically significant differences. Line thicknesses indicate the probability of a significant difference from the mean spreading index observed with LAT-reconstituted cells. In all cases, similar results were obtained in two independent experiments.

(see above, Figure 4). J.CaM2.5:WT cells treated with both BAPTA and EGTA also cluster actin within T cell-coverslip contacts, whereas similarly treated J.CaM2.5 cells do not (data not shown). To emphasize the effect of LAT on the calcium-independent clustering of actin, we replotted the spreading indices associated J.CaM2.5:WT and J.CaM2.5 cells treated with BAPTA and EGTA (Figure 6C). The small amount of actin reorganization that occurs in J.CaM2.5:WT cells produces a small, but significant, elevation in the spreading index relative to J.CaM2.5 cells, demonstrating that LAT promotes TCR-induced actin polymerization, even in the absence of intracellular calcium elevations.

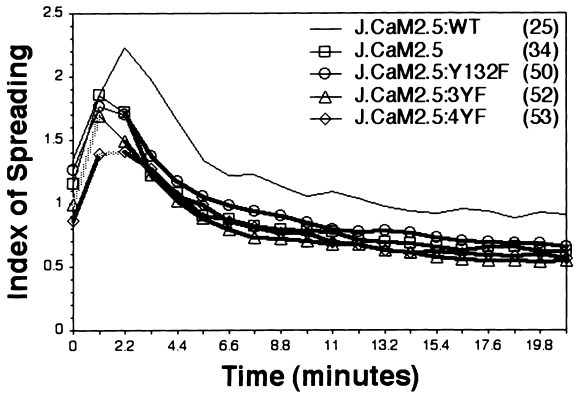

Figure 7. Both the PLCγ1 and Grb2/Gads Binding Sites in LAT Are Required for TCR-Induced Spreading

J.CaM2.5 cells reconstituted with variants of LAT and expressing EGFP-actin were plated onto UCHT1-coated coverslips. Cells were imaged and analyzed as in Figure 5; mean spreading indices are plotted here. Dotted and heavy lines, respectively, indicate that the probability of a significant difference from the mean spreading index observed with LAT-reconstituted cells is greater than 95% or 99%. Similar results were obtained in two independent experiments.

The PLCγ1 and Grb2/Gads Binding Sites in LAT Are Required for TCR-Induced Spreading

LAT couples to downstream effectors through phosphorylated tyrosine residues in its cytoplasmic tail. Four residues have been identified as playing critical roles in the transduction of signals downstream of LAT: tyrosines 132, 171, 191, and 226 (Zhang et al., 2000). To test whether or not these tyrosines are required for TCR-induced morphological changes, we performed spreading assays using EGFP-actin-expressing J.CaM2.5:4YF cells (Figure 7). These cells express a variant of LAT in which all four of these tyrosines have been converted to phenylalanine residues. Based on the indices of spreading, the behavior of these cells was indistinguishable from the behavior of J.CaM2.5 cells, suggesting that these four tyrosines, or some subset thereof, are required for the induction of normal morphological responses downstream of TCR engagement.

As shown above, normal T cell spreading requires LAT-dependent cytoplasmic calcium elevations. Notably, tyrosine 132 in the cytoplasmic tail of LAT is found in a consensus binding site for the SH2 domains of PLCγ1. The mutation of tyrosine 132 to phenylalanine (Y132F) abolishes the binding of PLCγ1 to LAT and prevents calcium entry downstream of LAT without affecting the ability of LAT to interact with Grb2 and Gads (Zhang et al., 2000). In addition, T cell spreading requires

actin polymerization, which may be directed by a complex of proteins associated with Gads and SLP-76 (referenced above). The three carboxy-terminal tyrosines in LAT, 171, 191, and 226, are in consensus binding sites for the SH2 domains of Grb2/Gads-related adaptors. The mutation of these three tyrosines to phenylalanine (3YF) prevents the binding of Grb2, Gads, and SLP-76 to LAT (Zhang et al., 2000). To test whether tyrosine 132 or the three carboxy-terminal tyrosines plays a role in the TCR-dependent induction of morphological changes, we performed spreading assays using EGFP-actin-expressing J.CaM2.5 cells reconstituted with either Y132F LAT or 3YF LAT (Figure 7). In both cases, the behavior of these cells was indistinguishable from the behavior of J.CaM2.5 cells, indicating that both sets of tyrosines are required for normal TCR-induced spreading.

Discussion

The crucial role of LAT with respect to the biochemical and transcriptional changes that accompany T cell activation has been well documented. However, dramatic and functional changes in cell shape and cytoskeletal organization also occur during T cell activation. Several components of LAT-nucleated signaling complexes have been observed to influence the organization of the T cell cytoskeleton, suggesting that LAT itself plays a critical role in these morphological changes. To determine the contribution of LAT to these structural changes, we developed methods that enabled us to visualize and quantitate the morphological responses of individual T cells over time.

Our approach to imaging the contacts formed in response to TCR ligation offers several major advantages. First, the simplified nature of the stimulus used here eliminates the complicating contributions of surface receptors other than the TCR to T cell spreading. Furthermore, the contacts produced in response to our coverslips may be better ordered and more symmetric than those observed on APCs in vivo, where the relevant antigenic MHC-peptide complexes are distributed randomly. We also expect the simplified nature of the stimulus to facilitate the adaptation of this assay to the study of dynamic changes in the distributions of EGFP-tagged signaling proteins in primary T cells. Second, unlike soluble antibodies, coverslip-bound antibodies cannot simultaneously engage all surface-exposed TCRs. In this regard, coverslip-bound antibodies mimic the early stages of physiological stimulation by providing a polarized stimulus and by requiring responding T cells to undergo morphological changes in order to bring TCRs to bear on the activating surface. By preserving this requirement for morphological change, our assay may reveal novel signaling requirements downstream of the TCR. Finally, our method constrains the contacts formed by activated T cells to a plane defined by a stimulatory coverslip and thereby facilitates the rapid collection of high-resolution images of the contact. The resulting images can be used to quantitate the extent of morphological change and cytoskeletal rearrangement in individual cells on an ongoing basis. This type of analysis permits more nuanced descriptions of the morphological changes induced by TCR ligation than assays in which morphological events are scored at fixed time points following stimulation. Given the complexity of the cytoskeletal processes controlled by TCR engagement, the identification of distinct pathways controlling TCR-dependent morphological changes may require the increased resolution provided by this assay.

The conditions of this assay differ from those prevailing during physiological contact formation in at least two important respects. First, we did not use primary T cells in these studies. Since T cells do not develop in the absence of LAT in vivo, this was unavoidable (Zhang et al., 1999c). However, spreading and actin ring formation are not peculiar to Jurkat T cells, as recent studies in our laboratory (C. L. Fuller and S. C. B., unpublished data) have demonstrated that murine cytotoxic T cells undergo similar cytoskeletal changes in response to immobilized stimulatory antibodies. Second, we used immobilized antibodies to the TCR rather than antigenic MHC-peptide complexes to stimulate T cells. Since these antibodies bind tightly to the TCR, the immobilized antibodies may prevent events characteristic of later phases of T cell activation, including the lateral redistribution of TCRs into c-SMACs and the internalization of TCRs. Nevertheless, many of the morphological responses observed in response to immobilized antibodies parallel those observed during the early stages of physiological contact formation: the extension of lamellipodia toward the stimulatory surface within seconds of contact, the flattening of cells, the formation of both circumferential adherent rings and actin-rich rings, and the reorientation of the MTOC toward the contact zone (Stowers et al., 1995; Negulescu et al., 1996; Delon et al., 1998; Wulfing et al., 1998; Grakoui et al., 1999).

Delon et al. (1998) demonstrated that actin polymerization is required for the formation of T cell-APC contacts. Our studies demonstrate that actin polymerization is also required for the expansion of T cell-coverslip contacts. We propose that actin polymerization drives the active expansion of contacts by enabling the extension of lamellipodia (Welch et al., 1997). Several observations support this view. For example, the initial contact between a filopodial structure on a T cell and the stimulatory coverslip triggers the projection of lamellipodia toward the coverslip. These lamellipodia contact the coverslip and attach tightly, increasing the size of the contact (Figure 1B). Subsequently, as the contact expands rapidly, large lamellipodia project outward from the contact, dramatically increasing the surface area covered by the responding T cell (Figure 2B). Furthermore, as the growth of the contact slows, lamellipodia are reduced in size (Figure 2B). Finally, for as long as the stable contact is maintained, lamellipodia extend from the perimeter of the responding T cell (see supplemental movie 3 at http://www.immunity.com/cgi/content/full/14/3/315/DC1; Figure 2C; data not shown). This model suggests that signaling proteins that promote actin polymerization and the extension of protrusive structures, such as Vav, Cdc42, Rac, and WASP, may enhance T cell activation, at least in part, by increasing the size of the contact and thereby increasing the likelihood of additional TCR engagements. In contrast, Borroto et al. (2000) have argued that Cdc42 and Rac do not play a role in TCR-induced spreading; however, their observations are based on images obtained 20 min

after the initiation of contact, at which point the dynamic expansion of the T cell-coverslip contact has ceased. This model may also explain the observation, made by Parsey and Lewis (1993), that inhibitors of actin polymerization block the activation of PTKs by immobilized TCR-specific antibodies.

Prior to this report, the contribution of MTOC polarization to contact formation had not been addressed directly. Our results demonstrate the ability of the microtubule cytoskeleton to stabilize contacts but preclude a primary role for the microtubule cytoskeleton in the initial expansion of contacts. Since the reorientation of the MTOC (3–5 min, data not shown) normally precedes the effects of microtubule disruption (after 7 min), the polarization of the microtubule cytoskeleton toward the coverslip may contribute to sustained spreading. We also observed that the effects of microtubule depolymerization are less severe than the effects of intracellular calcium chelation. This is consistent with reports that have demonstrated a role for calcium elevations in the reorientation of the MTOC (Kupfer et al., 1987; Lowin-Kropf et al., 1998). Finally, Delon et al. observed that the microtubule cytoskeleton promotes sustained calcium influxes, which we and others have shown to stabilize contacts (Negulescu et al., 1996; Delon et al., 1998). However, our results indicate that the microtubule cytoskeleton acts to stabilize contacts within 7 min, whereas the effects of calcium influxes do not become apparent until after 12 min. Additional mechanisms that may explain this stabilizing effect include the microtubule-dependent physical stabilization of the contact, the microtubule-dependent activation of Rac, or the microtubule-dependent reorganization of vesicular traffic (Matteoni and Kreis, 1987; Waterman-Storer et al., 1999).

Since the adaptor protein LAT governs several critical biochemical events downstream of the TCR, we chose to assess the role of LAT with respect to the morphological changes induced by TCR ligation. We expected that the absence of LAT would abolish T cell spreading. Instead, LAT-deficient cells produce actin-rich contacts, which, although less extensive, less well organized, and shorter lived than those formed by LAT-reconstituted cells, are significantly more extensive than those formed in the absence of either actin polymerization or cytoplasmic calcium increases. Closer examination revealed that small, transient calcium elevations do occur when LAT-deficient cells are plated on stimulatory coverslips and are crucial to the transient spreading responses of LAT-deficient cells. Nevertheless, the defects in the spreading responses of LAT-deficient T cells are quite severe. The impaired calcium responses of LAT-deficient T cells are likely to contribute to these defects, as these calcium responses are only marginally competent to induce transient bursts of spreading and cannot support sustained spreading. However, calcium-independent mechanisms also appear to be responsible for these spreading defects, as LAT-deficient cells fail to cluster actin within the T cell-coverslip contact in the absence of calcium elevations. Although we have not identified the effectors that mediate LAT-dependent spreading, SLP-76, Vav, Cdc42, Rac, Pak, and WASP may contribute to LAT-dependent morphological changes through effects on either the actin cytoskeleton or the microtubule cytoskeleton. In contrast, LAT-dependent ERK activation does not contribute to the TCR-dependent morphological changes observed in this study.

Although the absence of LAT does not completely abolish T cell spreading, our results confirm that tyrosine kinase activity is absolutely required for both the formation of contacts and T cell spreading (Delon et al., 1998; Borroto et al., 2000). This strongly suggests that transient changes in the organization of the actin cytoskeleton can be driven by TCR-proximal PTKs in the absence of LAT. These LAT-independent mechanisms could involve the recruitment of effectors such as PLCγ1 or Fyb/SLAP to either the TCR or TCR-associated PTKs (da Silva et al., 1997; Williams et al., 1999). Alternately, the residual levels of LAT remaining in J.CaM2.5 cells ($<$2% normal levels) may be sufficient to direct the weak responses observed here. We feel that this is unlikely, as 4YF LAT expressed at levels exceeding the residual level of LAT by 50-fold did not reproducibly suppress the spreading response observed in J.CaM2.5 cells.

We attempted to identify distinct signal transduction pathways contributing to T cell spreading by examining the spreading responses of LAT-deficient cells reconstituted with either Y132F, 3YF, or 4YF LAT. However, the morphological responses of these cells were indistinguishable from those of nonreconstituted LAT-deficient cells. This may result from the complexity of interactions at LAT that regulate these morphological changes. For example, although the Y132F mutation specifically eliminates the predicted PLCγ1 binding site in LAT and does not affect the recruitment of either Grb2 or Gads to LAT, this mutation substantially reduces the recruitment of SLP-76 to LAT (Zhang et al., 2000). Similarly, the 3YF mutation specifically eliminates the Grb2 and Gads binding sites in LAT without affecting the predicted PLCγ1 binding site but nevertheless reduces both the phosphorylation of PLCγ1 and the association of PLCγ1 with LAT (Zhang et al., 2000).

In this study, we have described an assay system that is capable of reproducing many of the morphological changes induced by stimulatory APCs and is compatible with several dynamic imaging techniques. Using this assay, we have shown that LAT plays an important role in the regulation of T cell spreading but does not govern all TCR-induced morphological changes. Unfortunately, the complex nature of effector recruitment to LAT prevented us from identifying signaling pathways responsible for distinct aspects of the spreading responses regulated by LAT. We expect to address these issues in the future by using this assay to explore the roles played by PTKs upstream of and effector molecules downstream of LAT.

Experimental Procedures

Materials

The murine monoclonal antibodies used in coverslip binding assays were obtained from Pharmingen (anti-CD3ϵ, UCHT1; anti-CD11a, HI111; anti-CD25, M-A251; anti-CD43, 1G10; and anti-CD71, M-A712) or were produced in the laboratory (anti-CD3ϵ, OKT3 ascites). The EGFP-actin expression vectors pEGFP-actin and pEYFP-actin were obtained from Clontech. RPMI 1640 was obtained from GIBCO BRL. Other tissue culture supplies were from Biofluids. Inhibitory compounds were obtained from Sigma Chemical Co. (cytochalasin D, colchicine, and EGTA) or from Calbiochem (PP2, PD98059, and BAPTA-AM). All other chemical reagents were from Sigma.

Cell Culture and the Generation of Stable Cell Lines

Jurkat E6.1, the LAT-deficient Jurkat-derivative J.CaM2.5, and reconstituted variants of J.CaM2.5 expressing wild-type LAT, Y132F LAT, 3YF LAT, and 4YF LAT have been described previously (Zhang et al., 2000). Cells were transfected with either pEGFP-actin or pEYFP-actin using a Bio-Rad Gene Pulser (Hercules, CA). EGFP-positive cells were selected using G418 selection, cell sorting (FACS-Calibur), and limiting dilution plating to isolate clones stably expressing EGFP-actin. TCR and LAT expression were confirmed by either surface staining or intracellular staining and flow cytometry.

Spreading Assays

Four-chambered coverglasses (LabTek) were cleaned by treatment with 1 M HCl, 70% ethanol for 30 min and dried at 60°C for 30 min. The chambers were treated with a 0.01% w/v poly-L-lysine solution (Sigma) for 5 min, drained, and dried at 60°C for 30 min. Purified antibodies in PBS (10 μg/ml) were bound to the coverslips for 3 hr at 37°C. Chambers were rinsed extensively in PBS and stored at 4°C. Responding cells were not allowed to exceed a density of 2×10^5 cells/ml for 2 days prior to spreading assays. Spreading assays were initiated by injecting 10 μl of a concentrated cell suspension (2×10^6 cells/ml) into the bottom of treated chambers containing normal culture medium supplemented with 25 mM Hepes.

Where indicated, Jurkat cells were preincubated at 37°C for 20 min prior to assay with either DMSO, cytochalasin D (10 μM), colchicine (100 μM), PP2 (10 μM), or PD98059 (50 μM); these drugs were also present in the imaging chamber. At these doses, cytochalasin D, PP2, and PD98059 inhibited TCR-induced actin polymerization, tyrosine phosphorylation, and ERK phosphorylation, respectively. Similarly, colchicine disrupted the microtubule cytoskeleton in EGFP-tubulin expressing Jurkat cells. To prevent calcium influx without depleting intracellular calcium stores, EGTA (1 mM) was present only in the imaging chamber. To prevent any elevation of intracellular calcium, cells were preloaded with BAPTA-AM (50 μM) for 20 min at 37°C in complete media buffered with 1 mM EGTA. BAPTA-loaded cells were rinsed and injected into chambers supplemented with EGTA (1 mM). The effectiveness of these treatments was confirmed using Jurkat cells loaded with intracellular calcium indicators.

Cellular Imaging

For time lapse imaging, chambers were mounted at 37°C on a temperature-controlled inverted microscope (Zeiss Axiovert 135TV) equipped with a 63× oil-immersion Plan-Apochromat objective (NA 1.4, Carl Zeiss). The acquisition of visible light and fluorescent images was performed using a SenSys 12-bit CCD camera (Photometrics, Ltd), a filter wheel, and a Z-drive (Ludl Electronic Products, Ltd) controlled by IP Lab 3.5 imaging software (Scanalytics, Inc.). Fluorescent images were collected using a DAPI/FITC/Texas-Red multiple-pass dichroic and emission filter and either the FITC (D490x) or Texas-Red (D570x) excitation filters (#8300, Chroma Technology Corp.). In Figure 2B, DiIC18(3) (DiI), a dialkylindocarbocyanine lipid analog, appears in both the FITC channel and the Texas-Red channel, resulting in the yellowish appearance of the DiI-positive vesicles. Confocal images were collected similarly using a LSM 410 confocal microscope (Carl Zeiss) equipped with an internal 633 nm laser and an external krypton/argon laser (Spectra-Physics). EGFP was imaged using the external 488 nm laser line in conjunction with a FT 488/568 dichroic (Carl Zeiss) and a BP 540/50 emission filter (Chroma). IRM images were collected using the 633 nm laser line in conjunction with a FT 633 dichroic and an open emission filter. Time-lapse sequences were recorded using a custom macro program that periodically focuses on the coverslip surface, captures confocal IRM and fluorescence images at the coverslip, and then captures a fluorescence image 5 μm above the coverslip.

Image Processing and the Index of Spreading

NIH Image 1.62 was used to sequentially shadow and smooth IRM images to enhance contrast. IP Lab 3.5 was used for all other image manipulations. The pseudocolored images in Figures 3–5 depict EGFP-actin fluorescence at the coverslip in red and EGFP-actin fluorescence in the cell body, 5 μm above the coverslip, in green.

The index of spreading is derived by taking the standard deviation of EGFP-actin pixel intensities at the coverslip and dividing by the standard deviation of EGFP-actin pixel intensities in the cell body. This ratio is independent of cell brightness and is positively correlated with the recruitment of actin to the coverslip and the expansion of the contact. The polymerization of actin into discrete structures at the coverslip also contributes to the index of spreading by increasing the number of bright and dark pixels at the expense of pixels of mean brightness.

Primary images of fields of cells were collected every 33 s. Images of individual cells were extracted from primary image stacks, and the resulting image sequences were synchronized for the time of initial contact with the coverslip, as assessed by confocal IRM. Spreading indices were calculated for each image. Plots of the spreading index versus time were smoothed by averaging data points in a pairwise manner. The extraction of individual cells and the derivation of the corresponding spreading indices were automated using IP Lab.

Mean spreading indices were determined for populations of cells according to cell type or pharmacological treatment. The number of cells in each population is shown in parentheses and line thickness indicates the probability of a significant difference from the indicated control group as assessed by a one-tailed t-test. Population means and measurements of statistical significance were calculated using Microsoft Excel.

Acknowledgments

We acknowledge G. F. Vande Woude for his support, J. S. Bonifacino, P. L. Schwartzberg, and J. E. van Leeuwen for critical reading of this manuscript, and J. Lippincott-Schwartz for the use of the confocal microscope. We also thank D.P. Bottaro and the members of J. Lippincott-Schwartz's laboratory for training in the use of epifluorescence and confocal microscopes. S. C. B. is supported by an award from the Cancer Research Institute; W. Z. was supported by an award from the Leukemia Society of America.

Received February 9, 2000; revised February 7, 2001.

References

Borroto, A., Gil, D., Delgado, P., Vicente-Manzanares, M., Alcover, A., Sanchez-Madrid, F., and Alarcon, B. (2000). Rho regulates T cell receptor ITAM-induced lymphocyte spreading in an integrin-independent manner. Eur. J. Immunol. *30*, 3403–3410.

Bubeck Wardenburg, J., Pappu, R., Bu, J.Y., Mayer, B., Chernoff, J., Straus, D., and Chan, A.C. (1998). Regulation of PAK activation and the T cell cytoskeleton by the linker protein SLP-76. Immunity *9*, 607–616.

Cantrell, D. (1998). Lymphocyte signalling: a coordinating role for Vav? Curr. Biol. *8*, R535–R538.

Chan, A.C., and Shaw, A.S. (1996). Regulation of antigen receptor signal transduction by protein tyrosine kinases. Curr. Opin. Immunol. *8*, 394–401.

Cheresh, D.A., Leng, J., and Klemke, R.L. (1999). Regulation of cell contraction and membrane ruffling by distinct signals in migratory cells. J. Cell Biol. *146*, 1107–1116.

Costello, P.S., Walters, A.E., Mee, P.J., Turner, M., Reynolds, L.F., Prisco, A., Sarner, N., Zamoyska, R., and Tybulewicz, V.L. (1999). The Rho-family GTP exchange factor Vav is a critical transducer of T cell receptor signals to the calcium, ERK, and NF-kappaB pathways. Proc. Natl. Acad. Sci. USA *96*, 3035–3040.

da Silva, A.J., Li, Z., de Vera, C., Canto, E., Findell, P., and Rudd, C.E. (1997). Cloning of a novel T-cell protein FYB that binds FYN and SH2-domain-containing leukocyte protein 76 and modulates interleukin 2 production. Proc. Natl. Acad. Sci. *94*, 7493–7498.

Delon, J., Bercovici, N., Liblau, R., and Trautmann, A. (1998). Imaging antigen recognition by naive CD4+ T cells: compulsory cytoskeletal alterations for the triggering of an intracellular calcium response. Eur. J. Immunol. *28*, 716–729.

Derry, J.M.J., Ochs, H.D., and Francke, U. (1994). Isolation of a novel gene mutated in Wiskott-Aldrich Syndrome. Cell *78*, 635–644.

Dudley, D.T., Pang, L., Decker, S.J., Bridges, A.J., and Saltiel, A.R. (1995). A synthetic inhibitor of the mitogen-activated protein kinase cascade. Proc. Natl. Acad. Sci. USA *92*, 7686–7689.

Dustin, M.L., and Cooper, J.A. (2000). The immunological synapse and the actin cytoskeleton: molecular hardware for T cell signaling. Nat. Immunol. *1*, 23–29.

Edwards, D.C., Sanders, L.C., Bokoch, G.M., and Gill, G.N. (1999). Activation of LIM-kinase by Pak1 couples Rac/Cdc42 GTPase signalling to actin cytoskeletal dynamics. Nat. Cell. Biol. *1*, 253–259.

Fincham, V.J., James, M., Frame, M.C., and Winder, S.J. (2000). Active ERK/MAP kinase is targeted to newly forming cell-matrix adhesions by integrin engagement and v-Src. EMBO J. *19*, 2911–2923.

Finco, T.S., Kadlecek, T., Zhang, W., Samelson, L.E., and Weiss, A. (1998). LAT is required for TCR-mediated activation of PLCγ1 and the Ras pathway. Immunity *9*, 617–626.

Fischer, K.D., Kong, Y.Y., Nishina, H., Tedford, K., Marengere, L.E., Kozieradzki, I., Sasaki, T., Starr, M., Chan, G., Gardener, S., et al. (1998). Vav is a regulator of cytoskeletal reorganization mediated by the T- cell receptor. Curr. Biol. *8*, 554–562.

Grakoui, A., Bromley, S.K., Sumen, C., Davis, M.M., Shaw, A.S., Allen, P.M., and Dustin, M.L. (1999). The immunological synapse: a molecular machine controlling T cell activation. Science *285*, 221–227.

Holsinger, L.J., Graef, I.A., Swat, W., Chi, T., Bautista, D.M., Davidson, L., Lewis, R.S., Alt, F.W., and Crabtree, G.R. (1998). Defects in actin-cap formation in Vav-deficient mice implicate an actin requirement for lymphocyte signal transduction. Curr. Biol. *8*, 563–572.

Krause, M., Sechi, A.S., Konradt, M., Monner, D., Gertler, F.B., and Wehland, J. (2000). Fyn-binding protein (Fyb)/SLP-76-associated protein (SLAP), Ena/vasodilator-stimulated phosphoprotein (VASP) proteins and the Arp2/3 complex link T cell receptor (TCR) signaling to the actin cytoskeleton. J. Cell Biol. *149*, 181–194.

Kupfer, A., and Dennert, G. (1984). Reorientation of the microtubule-organizing center and the golgi apparatus in cloned cytotoxic lymphocytes triggered by binding to lysable target cells. J. Immunol. *133*, 2762–2766.

Kupfer, A., Swain, S.L., and Singer, S.J. (1987). The specific direct interaction of helper T cells and antigen-presenting B cells. II. Reorientation of the microtubule organizing center and reorganization of the membrane-associated cytoskeleton inside the bound helper T cells. J. Exp. Med. *165*, 1565–1580.

Kupfer, H., Monks, C.R., and Kupfer, A. (1994). Small splenic B cells that bind to antigen-specific T helper (Th) cells and face the site of cytokine production in the Th cells selectively proliferate: immunofluorescence microscopic studies of Th-B antigen-presenting cell interactions. J. Exp. Med. *179*, 1507–1515.

Liu, K., Bunnell, S.C., Gurniak, C.B., and Berg, L.J. (1998). TCR-initiated calcium release is uncoupled from capacitative calcium entry in Itk-deficient T cells. J. Exp. Med. *187*, 1721–1727.

Liu, S.K., Fang, N., Koretzky, G.A., and McGlade, C.J. (1999). The hematopoietic-specific adaptor protein Gads functions in T-cell signaling via interactions with the SLP-76 and LAT adaptors. Curr. Biol. *9*, 67–75.

Lowin-Kropf, B., Shapiro, V.S., and Weiss, A. (1998). Cytoskeletal polarization of T cells is regulated by an immunoreceptor tyrosine-based activation motif-dependent mechanism. J. Cell Biol. *140*, 861–871.

Matteoni, R., and Kreis, T.E. (1987). Translocation and clustering of endosomes and lysosomes depends on microtubules. J. Cell Biol. *105*, 1253–1265.

Monks, C.R., Freiberg, B.A., Kupfer, H., Sciaky, N., and Kupfer, A. (1998). Three-dimensional segregation of supramolecular activation clusters in T cells. Nature *395*, 82–86.

Negulescu, P.A., Krasieva, T.B., Khan, A., Kerschbaum, H.H., and Cahalan, M.D. (1996). Polarity of T cell shape, motility, and sensitivity to antigen. Immunity *4*, 421–430.

Nobes, C.D., and Hall, A. (1999). Rho GTPases control polarity, protrusion, and adhesion during cell movement. J. Cell Biol. *144*, 1235–1244.

Parsey, M.V., and Lewis, G.K. (1993). Actin polymerization and pseudopod reorganization accompany anti-CD3 induced growth arrest in Jurkat T cells. J. Immunol. *151*, 1881–1893.

Scharenberg, A.M., and Kinet, J.P. (1998). PtdIns-3,4,5-P3: a regulatory nexus between tyrosine kinases and sustained calcium signals. Cell *94*, 5–8.

Sedwick, C.E., Morgan, M.M., Jusino, L., Cannon, J.L., Miller, J., and Burkhardt, J.K. (1999). TCR, LFA-1, and CD28 play unique and complementary roles in signaling T cell cytoskeletal reorganization. J. Immunol. *162*, 1367–1375.

Shan, X., and Wange, R.L. (1999). Itk/Emt/Tsk activation in response to CD3 cross-linking in Jurkat T cells requires ZAP-70 and Lat and is independent of membrane recruitment. J. Biol. Chem. *274*, 29323–29330.

Stewart, M.P., McDowall, A., and Hogg, N. (1998). LFA-1-mediated adhesion is regulated by cytoskeletal restraint and by a Ca2+-dependent protease, calpain. J. Cell Biol. *140*, 699–707.

Stowers, L., Yelon, D., Berg, L.J., and Chant, J. (1995). Regulation of the polarization of T cells toward antigen-presenting cells by Ras-related GTPase CDC42. Proc. Natl. Acad. Sci. USA *92*, 5027–5031.

Symons, M., Derry, J.M., Karlak, B., Jiang, S., Lemahieu, V., McCormick, F., Francke, U., and Abo, A. (1996). Wiskott-Aldrich syndrome protein, a novel effector for the GTPase CDC42Hs, is implicated in actin polymerization. Cell *84*, 723–734.

Valitutti, S., Dessing, M., Aktories, K., Gallati, H., and Lanzavecchia, A. (1995). Sustained signaling leading to T cell activation results from prolonged T cell receptor occupancy. Role of T cell actin cytoskeleton. J. Exp. Med. *181*, 577–584.

Wange, R.L., and Samelson, L.E. (1996). Complex complexes: signaling at the TCR. Immunity *5*, 197–205.

Waterman-Storer, C.M., Worthylake, R.A., Liu, B.P., Burridge, K., and Salmon, E.D. (1999). Microtubule growth activates Rac1 to promote lamellipodial protrusion in fibroblasts. Nat. Cell Biol. *1*, 45–50.

Welch, M.D., Mallavarapu, A., Rosenblatt, J., and Mitchison, T.J. (1997). Actin dynamics in vivo. Curr. Opin. Cell Biol. *9*, 54–61.

Williams, B.L., Irvin, B.J., Sutor, S.L., Chini, C.C.S., Yacyshyn, E., Bubeck Wardenburg, J., Dalton, M., Chan, A.C., and Abraham, R.T. (1999). Phosphorylation of Tyr319 in ZAP-70 is required for T-cell antigen receptor-dependent phospholipase C-γ1 and Ras activation. EMBO J. *18*, 1832–1844.

Wu, J., Motto, D.G., Koetzky, G.A., and Weiss, A. (1996). Vav and SLP-76 interact and functionally cooperate in IL-2 gene activation. Immunity *4*, 593–602.

Wulfing, C., and Davis, M.M. (1998). A receptor/cytoskeletal movement triggered by costimulation during T cell activation. Science *282*, 2266–2269.

Wulfing, C., Sjaastad, M.D., and Davis, M.M. (1998). Visualizing the dynamics of T cell activation: intracellular adhesion molecule 1 migrates rapidly to the T cell/B cell interface and acts to sustain calcium levels. Proc. Natl. Acad. Sci. USA *95*, 6302–6307.

Yablonski, D., Kuhne, M.R., Kadlecek, T., and Weiss, A. (1998). Uncoupling of nonreceptor tyrosine kinases from PLC-gamma1 in an SLP-76-deficient T cell. Science *281*, 413–416.

Zhang, W., and Samelson, L.E. (2000). The role of membrane-associated adaptors in T cell receptor signalling. Semin. Immunol. *12*, 35–41.

Zhang, W., Sloan-Lancaster, J., Kitchen, J., Trible, R.P., and Samelson, L.E. (1998a). LAT: the ZAP-70 tyrosine kinase substrate that links T cell receptor to cellular activation. Cell *92*, 83–92.

Zhang, W., Trible, R.P., and Samelson, L.E. (1998b). LAT palmitoylation: its essential role in membrane microdomain targeting and tyrosine phosphorylation during T cell activation. Immunity *9*, 239–246.

Zhang, J., Shehabeldin, A., da Cruz, L.A., Butler, J., Somani, A.K., McGavin, M., Kozieradzki, I., dos Santos, A.O., Nagy, A., Grinstein, S., et al. (1999a). Antigen receptor-induced activation and cytoskele-

tal rearrangement are impaired in Wiskott-Aldrich syndrome protein-deficient lymphocytes. J. Exp. Med. *190*, 1329–1342.

Zhang, W., Irvin, B.J., Trible, R.P., Abraham, R.T., and Samelson, L.E. (1999b). Functional analysis of LAT in TCR-mediated signaling pathways using a LAT-deficient Jurkat cell line. Int. Immunol. *11*, 943–950.

Zhang, W., Sommers, C.L., Burshtyn, D.N., Stebbins, C.C., DeJarnette, J.B., Trible, R.P., Grinberg, A., Tsay, H.C., Jacobs, H.M., Kessler, C.M., et al. (1999c). Essential role of LAT in T cell development. Immunity *10*, 323–332.

Zhang, W., Trible, R.P., Zhu, M., Liu, S.K., McGlade, C.J., and Samelson, L.E. (2000). Association of Grb2, Gads, and phospholipase C-gamma 1 with phosphorylated LAT tyrosine residues. Effect of LAT tyrosine mutations on T cell angigen receptor-mediated signaling. J. Biol. Chem. *275*, 23355–23361.

Zigmond, S.H. (2000). How WASP regulates actin polymerization. J. Cell Biol. *150*, F117–F120.